

# On the Reaction of 2,4,5-Trichlorophenol with Hydroxyl Radicals: New Information on Transients and Their Properties

Marija Bonifačić,<sup>†</sup> Klaus-Dieter Asmus,<sup>‡</sup> and Kimberly A. Gray<sup>\*,§</sup>

Department of Physical Chemistry, Ruđer Bošković Institute, Bijenička c. 54, 10000 Zagreb, Croatia, Faculty of Chemistry, Adam-Mickiewicz-University, Grunwaldzka 6, 60-780 Poznan, Poland, and Department of Civil and Environmental Engineering, Northwestern University, 2145 Sheridan Road, Evanston, Illinois 60208-3109

Received: July 26, 2002; In Final Form: October 24, 2002

A reinvestigation of the  $\bullet\text{OH}$  radical reaction with 2,4,5-trichlorophenol (TCP) provided unambiguous direct evidence, in contrast to an earlier study, for the formation of two different  $\bullet\text{OH}$ -adducts, namely, at the C-6 and C-3 positions. They appear to be formed at about equal yield and exhibit different optical absorption spectra with maxima at 320 and 350 nm for the C-6 adduct and 320 nm for the C-3 adduct. Both are mild reductants as can be deduced from their reaction with  $\text{Fe}(\text{CN})_6^{3-}$ . Owing to its relatively low  $\text{p}K_{\text{a}}$  ( $4.8 \pm 1$ ), the C-6-adduct reacts in neutral to slightly acid solutions preferentially through its deprotonated form. Absolute rate constants have been measured for the reduction of  $\text{Fe}(\text{CN})_6^{3-}$  by the anion of the 6-hydroxy adduct radical ( $1.4 \pm 0.3$ )  $\times 10^8 \text{ M}^{-1} \text{ s}^{-1}$  and by the neutral form of the 3-hydroxy adduct radical ( $2.7 \pm 0.6$ )  $\times 10^6 \text{ M}^{-1} \text{ s}^{-1}$ . The latter assignment corrects the previous conclusion that attributed the low  $10^6 \text{ M}^{-1} \text{ s}^{-1}$  order of magnitude rate constant to the reaction of the C-6 adduct radical. Based on the reduction kinetics measurements, the rate constant for the C-6 adduct radical deprotonation process has been estimated to be about  $3 \times 10^4 \text{ s}^{-1}$ . The C-6-adduct, both in its neutral as well as in its anionic form, gains particular stability through hydrogen bond bridging between the two hydroxyl groups positioned at C-6 and C-1, and this accounts for the elevated rates that we report.

## Introduction

Reactions of halogenated phenols with hydroxyl radicals have been the subject of many investigations and, using the time-resolved technique of pulse radiolysis, several mechanistic aspects have been revealed.<sup>1–6</sup> Because a major class of environmental pollutants are halogenated phenolic compounds, there is strong interest in acquiring mechanistic information about the oxidative transformation of these compounds. This knowledge will promote the development of effective remediation strategies based on radical reactions and the formulation of kinetic models to predict the types of products formed under various chemical conditions.<sup>7</sup>

An extensive and elaborate study concerning 2,4,5-trichlorophenol,  $\text{Cl}_3\text{C}_6\text{H}_2\text{OH}$ , (TCP) was conducted by Draper et al.<sup>3</sup> Their main findings include, among others, a spectral characterization of a transient  $\bullet\text{OH}$  radical adduct to TCP, i.e., a dihydroxycyclohexadienyl-type radical. Its absorption spectrum was reported to exhibit a peak at 320 nm ( $\epsilon = 5300 \text{ M}^{-1} \text{ cm}^{-1}$ ) with an indication of a possible small shoulder at around 350 nm. Chemically, this transient was identified as a mild reductant on the basis of its reactions with the powerful electron acceptors  $\text{IrCl}_6^{2-}$  ( $E^\circ +1.02 \text{ V}$ ) and  $\text{Fe}(\text{CN})_6^{3-}$  ( $E^\circ +0.36 \text{ V}$ ) and associated relatively low rate constants of  $4.9 \times 10^7$  and  $\approx 10^6 \text{ M}^{-1} \text{ s}^{-1}$ , respectively. Structurally, the species was assigned to the 6-hydroxy adduct **A** $\bullet$ , in preference over the 3-hydroxy adduct **B** $\bullet$ , supported by an AM1 calculation of the respective

heats of formation (slightly more negative for **A** $\bullet$ ). Furthermore, these studies revealed a relatively low  $\text{p}K_{\text{a}} = 4.8$  for the  $\bullet\text{OH}$ -adduct radical.

In a routine reinvestigation of this TCP system, originally simply seeking to confirm these earlier data, we came across a number of additional facts and conclusions that, we feel, justify this complementing report. In particular, we can now present direct evidence for the 3-hydroxy adduct radical **B** $\bullet$ , formed in yields comparable with **A** $\bullet$  (for structures see Scheme 1). It is further shown how the redox properties of both transients depend on the pH, especially the first  $\text{p}K_{\text{a}}$  of the dihydroxy transient radical. The structural conclusions are supported by kinetic data on  $\text{Fe}(\text{CN})_6^{3-}$  reduction by the adduct radicals and on the protonation of the anionic form of the dihydroxy species.

## Experimental Section

All investigations were conducted in aqueous solution. The water was purified by the Serv-A-Pure Co. system. 2,4,5-Trichlorophenol (TCP) and other chemicals were used as received from the vendors (Aldrich, Fluka). Adjustments of pH were achieved by adding appropriate amounts of suitable  $\text{HClO}_4$  or  $\text{NaOH}$  solutions.

Pulse radiolysis was performed with an 8 MeV Titan Beta model TBS-8/16-1S LINAC at the Notre Dame Radiation Laboratory with pulses of 2.5 ns duration and doses per pulse in the range of 2–10 Gy. A description of the pulse radiolysis setup, data collection, and processing can be found elsewhere.<sup>8</sup> Solutions were generally deaerated and saturated with  $\text{N}_2\text{O}$ . Under these conditions, approximately 90% of all primary species available for reaction with the solute TCP were  $\bullet\text{OH}$  radicals. The remaining  $\approx 10\%$  are  $\text{H}\bullet$  atoms, and for their yield,

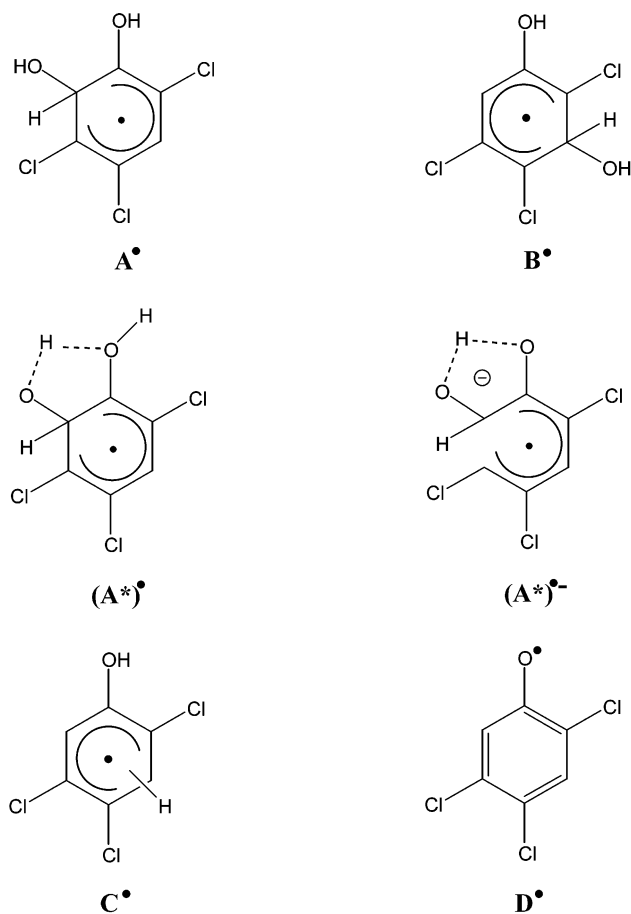
\* To whom correspondence should be addressed. E-mail: k-gray@northwestern.edu.

<sup>†</sup> Ruđer Bošković Institute.

<sup>‡</sup> Adam-Mickiewicz-University.

<sup>§</sup> Northwestern University.

## SCHEME 1



a value of  $G(\text{H}^{\bullet}) = 0.06 \mu\text{mol J}^{-1}$  was used. The yield of scavengable hydroxyl radicals,  $G(\text{OH}^{\bullet})$ , was calculated by taking into account the total concentration of TCP and the rate constant for the TCP reaction with hydroxyl radicals ( $1.2 \times 10^{10} \text{ M}^{-1} \text{ s}^{-1}$ )<sup>3</sup> according to a generally applicable formula.<sup>9</sup> The total concentration of  $\text{OH}^{\bullet}$  radicals per pulse applied in our present investigation of  $\text{N}_2\text{O}$ -saturated systems amounts to about 1–6  $\mu\text{M}$ . Dosimetry was performed with thiocyanate solutions as described earlier.<sup>10</sup>

Error limits of radiation chemical experiments are generally considered to be about  $\pm 10\%$ . They apply also to our present set of data unless specifically noted. All experiments have been conducted at room temperature.

## Results and Discussion

**Optical Spectra.** Figure 1a shows the transient absorption spectrum observable 5  $\mu\text{s}$  after application of a pulse of radiation (dose: ca. 3 Gy) to a deoxygenated,  $\text{N}_2\text{O}$ -saturated aqueous solution, pH 3.2, containing 3 mM TCP and 0.18 mM  $\text{Fe}(\text{CN})_6^{3-}$ . The choice of these experimental conditions was made to provide comparable conditions to the study conducted earlier by Draper et al.<sup>3</sup> In particular, they were set to ensure complete scavenging of the hydroxyl radicals by the halogenated phenol, and an observable secondary reaction of the transient formed in this initial process with the electron donor hexacyanoferrate (III). The relatively low pH of 3.2 was selected to keep TCP ( $\text{p}K_{\text{a}} = 7.4$ ) and its product radicals protonated. The 5  $\mu\text{s}$ -transient spectrum, as shown in Figure 1a, did not change if the  $\text{Fe}(\text{CN})_6^{3-}$  was omitted. Differences became, of course, apparent for the decay kinetics.

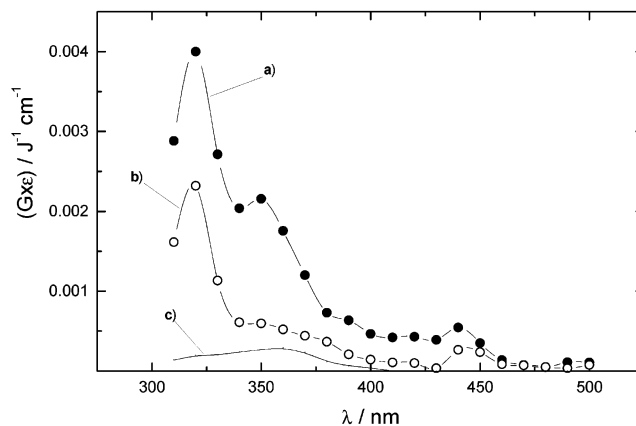


**Figure 1.** Absorption spectra measured 5  $\mu\text{s}$  (●) and 170  $\mu\text{s}$  (○) after the pulse irradiation of an  $\text{N}_2\text{O}$ -saturated aqueous solution containing 3 mM TCP and 0.18 mM  $\text{Fe}(\text{CN})_6^{3-}$  at pH 3.2. The no-symbol curve (c) shows the spectrum of the H-atom adduct, calculated by assuming  $G = 6 \times 10^{-8} \text{ mol J}^{-1}$  and  $\epsilon_{(360\text{nm})} = 4700 \text{ M}^{-1} \text{ cm}^{-1}$ .

The transient spectrum exhibits a pronounced maximum at 320 nm and a smaller second peak at 350 nm. Qualitatively, it resembles very well the spectrum published by Draper et al., which these authors assigned to the  $\text{OH}^{\bullet}$  radical adduct of TCP, i.e., the dihydroxy-trichloro-cyclohexadienyl radical **A•**.<sup>3</sup> From a quantitative point of view, however, it is noted that the 350 nm band is much more distinct in our present study than in the earlier work where it expressed itself as a small shoulder if any and, thus, escaped any further attention. The spectrum also exhibits some further features in the 370–470 nm range that warrant some discussion.

The improvement in spectral resolution can simply be attributed to the much higher sensitivity of the pulse radiolysis detection system used in our current study as compared to what was available in Draper's investigation. Before we focus further on the 320 and 350 nm bands and the possible involvement of the dihydroxy species **A•** and **B•**, let us briefly discuss two other radicals that are also unquestionably formed and contribute to the low energy side of the transient spectrum. The first of these is the H-atom side of the transient spectrum. The first of these is the H-atom adduct **C•**. Its yield amounts to  $G = G(\text{H}^{\bullet}) = 0.06 \mu\text{mol J}^{-1}$ , i.e., approximately 10% of the yield of radicals derived from  $\text{OH}^{\bullet}$  reaction ( $G(\text{OH}^{\bullet}) = 0.61 \mu\text{mol J}^{-1}$  in  $\text{N}_2\text{O}$ -saturated solutions containing 3 mM TCP). Radical **C•** (Scheme 1) exhibits maximum absorption at 360 nm and has been well characterized in the Draper et al. study. Taking its extinction coefficient of  $\epsilon = 4700 \text{ M}^{-1} \text{ cm}^{-1}$  the complete contribution of **C•** to the spectrum is represented by curve c in Figure 1. As can be seen, it is relatively insignificant, and therefore, it is not very meaningful to speculate on whether **C•** is a C-3 or C-6 adduct.

Attention is also drawn to the remaining small absorption peak at around 440 nm. This peak is typical of phenoxyl radicals (radical **D•** in case of TCP, see Scheme 1). There are two major modes by which the formation of this species can be rationalized. One is direct abstraction of a hydrogen atom by  $\text{OH}^{\bullet}$  from the phenolic hydroxyl group; an alternative pathway could proceed via an addition of  $\text{OH}^{\bullet}$  to the C-1 position and subsequent elimination of water from the transitory  $>\text{C}(\text{OH})_2$  group. It is not possible to distinguish between these two alternatives. Supporting evidence for the phenoxyl identity is drawn from the relatively long lifetime of the absorption in the 420–450 nm with an apparent second-order contribution in the decay kinetics. The total absorption measured at 430 nm amounts to  $(G \times \epsilon)_{430} = 5 \times 10^{-4} \text{ J}^{-1} \text{ cm}^{-1}$ . Assuming that **D•** is the only absorbing species in this wavelength range and taking

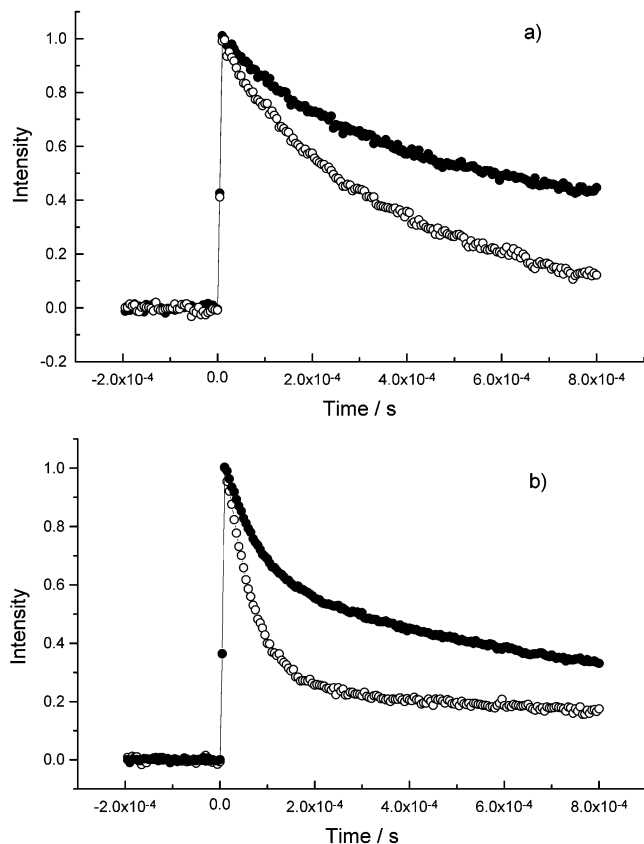


**Figure 2.** Absorption vs time traces taken at 320 nm (●) and 350 nm (○) in the pulse irradiated N<sub>2</sub>O-saturated aqueous solution at pH 3.2 containing 3 mM TCP (a) without and (b) in the presence of 0.18 mM Fe(CN)<sub>6</sub><sup>3-</sup>. Trace intensities are normalized to unity. Dose per pulse 3 Gy.

the known extinction coefficient of the phenoxyl radical of  $\epsilon = 3.6 \times 10^3 \text{ M}^{-1} \text{ cm}^{-1}$ , the yield is calculated at  $G = 0.14 \mu\text{mol J}^{-1}$ . This corresponds to ca. 23% of the available  $\cdot\text{OH}$  radicals, indicating that approximately one-fourth of all hydroxyl radicals, at most, end up as the phenoxyl radical.

The fact that at least two different adducts are formed in a solution containing only TCP (no Fe(CN)<sub>6</sub><sup>3-</sup> added) is indicated by a visibly significant difference in the decay kinetics of the absorption traces at 320 and 350 nm, respectively, as shown in Figure 2a. The kinetics followed second-order rate laws, i.e., responded with shorter half-lives upon increasing dose. The traces shown in Figure 2 refer to an identical dose per pulse (3 Gy) at both wavelengths. The intensities were normalized to unity for easier comparison. An even more striking difference was obtained when Fe(CN)<sub>6</sub><sup>3-</sup> was added to the solution. This is demonstrated in Figure 2b, for [Fe(CN)<sub>6</sub><sup>3-</sup>] = 0.18 mM. At both wavelengths, the presence of Fe(CN)<sub>6</sub><sup>3-</sup> caused an acceleration of the decay at early times compared to the Fe(CN)<sub>6</sub><sup>3-</sup>-free system. On the other hand, part of the overall intensity remained much longer-lived and practically unchanged upon the addition of Fe(CN)<sub>6</sub><sup>3-</sup> at this relatively low concentration. The ratio of the fast vs slow decay components, in terms of absorption intensity, amounts to about 3:1 at 350 nm and only 1:1 at 320 nm. A spectrum taken in the same Fe(CN)<sub>6</sub><sup>3-</sup> solution at 170  $\mu\text{s}$ , where the fast decay was essentially complete, is shown in Figure 1b. It can be seen that the shoulder at 350 nm has disappeared almost completely and that at this time the persisting absorption has a single maximum at 320 nm.

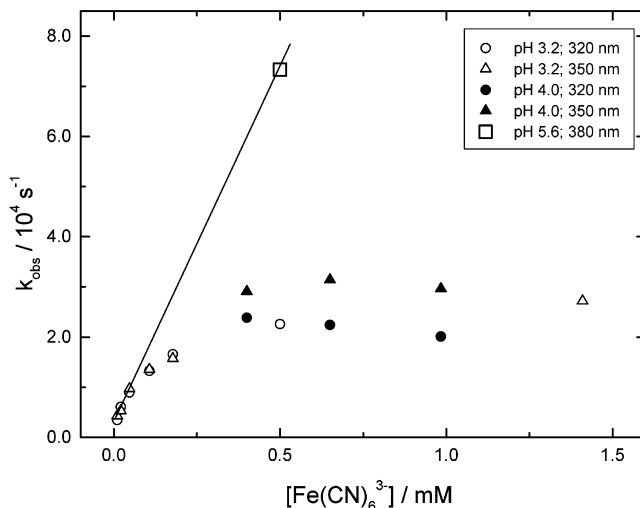


**Figure 3.**  $k_{\text{obs}}$  vs [Fe(CN)<sub>6</sub><sup>3-</sup>] for the “fast” decay part of the optical absorption traces measured at 320, 350, and 380 nm in pulse irradiated, N<sub>2</sub>O-saturated aqueous solutions containing 3 mM TCP, at pH 3.2, 4.0, and 5.6.

**Fe(CN)<sub>6</sub><sup>3-</sup> Reduction. Kinetics.** Further important information is obtained from the Fe(CN)<sub>6</sub><sup>3-</sup> reduction kinetics. In principle, all three reducing radicals A $\cdot$ , B $\cdot$ , and C $\cdot$  must be considered although the contribution of the H-atom adduct C $\cdot$  will be relatively small. The major processes are expected to reflect reduction reactions by the  $\cdot\text{OH}$ -adducts A $\cdot$  and B $\cdot$ . Decay curves such as shown in Figure 2b were generally analyzed by fitting to double exponentials. This allowed separate analysis of the two components and the evaluation of the pseudo-first-order rate constants ( $k_{\text{obs}}$ ) for each individual process. At lower Fe(CN)<sub>6</sub><sup>3-</sup> concentrations ( $\leq 0.2$  mM), the second-order radical-radical reaction(s) appeared to contribute to some extent to the overall decay rate of the slower process. Data for these systems were, therefore, analyzed only for the initial, fast part of the kinetics. Also, to keep the second-order contribution as low as possible, all experiments for kinetic evaluation were performed at a constant and relatively low dose per pulse of about 3 Gy.

The kinetics of the fast decay process observed at 320 and 350 nm was measured at two pHs (3.2 and 4.0) as a function of Fe(CN)<sub>6</sub><sup>3-</sup> concentration. The results, in terms of first-order rate constants  $k_{\text{obs}}$ , are plotted in Figure 3. Obviously, the overall kinetics reflects a complex process and, yet, still reveals some interesting features. Linear dependency with a positive slope in the  $k_{\text{obs}}$  vs [Fe(CN)<sub>6</sub><sup>3-</sup>] plot exists only at low, i.e.,  $\leq 10^{-4}$  M, electron acceptor concentration, and at [Fe(CN)<sub>6</sub><sup>3-</sup>]  $\geq 4 \times 10^{-4}$  M, a plateau region is attained at a rate constant of  $k_{\text{obs}} = (2.8 \pm 0.6) \times 10^4 \text{ s}^{-1}$ . Furthermore, there are hardly any differences noticeable between the pH 3.2 and 4.0 and between the 320 and 350 nm data. In particular, in the pH 4.0 experiments, the seemingly slightly higher 350 nm plateau values compared to those at 320 nm should not be over-interpreted because the observed differences can fully be accommodated within the experimental limits of error. In any case, the plateau shows that the formation of the reducing species becomes the rate determining process for the Fe(CN)<sub>6</sub><sup>3-</sup> reduction at higher scavenger concentrations.

When the pH was increased to 5.6, the picture changed significantly. At this pH and [Fe(CN)<sub>6</sub><sup>3-</sup>] = 0.5 mM, the initial decay was considerably accelerated compared with pH 3.2. The obtained value for  $k_{\text{obs}}$  fits now very well the straight-line obtained at pH 3.2 and [Fe(CN)<sub>6</sub><sup>3-</sup>]  $\leq 0.1$  mM (see Figure 3). It is important to note that this last set of experiments was

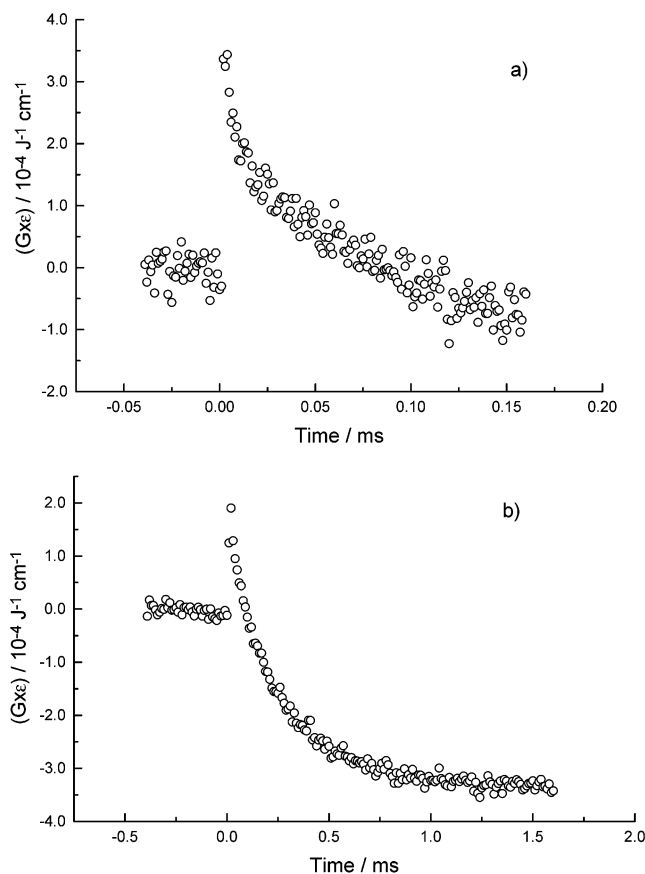


**Figure 4.** Absorption (shown in  $G \times \epsilon$  units) vs time trace recorded at 420 nm in pulse irradiated  $\text{N}_2\text{O}$ -saturated aqueous solution at pH 4.0, containing 3 mM TCP and 1 mM  $\text{Fe}(\text{CN})_6^{3-}$  shown on (a) 0.2 ms and (b) 2.0 ms time scale. Doses per pulse 3 Gy.

conducted well above the  $\text{p}K_a = 4.8$  attributed to  $\text{A}^{\cdot 3}$ . Because the monoanionic form of this transient (one of the two hydroxyl groups deprotonated) exhibits an absorption maximum at 380 nm, the pH 5.6 measurements were conducted at this more red-shifted wavelength.

The second-order rate constant derived from the slope of the straight line shown in Figure 3, and being common to pHs 3.2 and 5.6, amounts to  $(1.4 \pm 0.3) \times 10^8 \text{ M}^{-1} \text{ s}^{-1}$ . This value is 2 orders of magnitude higher than the one published ( $\approx 10^6 \text{ M}^{-1} \text{ s}^{-1}$ ) for the reduction of  $\text{Fe}(\text{CN})_6^{3-}$  by the presumed 6-hydroxyl adduct radical  $\text{A}^{\cdot 3}$  and determined from the kinetics of  $\text{Fe}(\text{CN})_6^{3-}$  bleaching at 420 nm in Draper's paper.<sup>3</sup> To resolve this significant difference, we also checked the kinetics at 420 nm. Our results, in terms of absorption–time traces at two different time scales, are displayed in Figure 4, parts a and b. They show, first of all, that there is not only bleaching at 420 nm but also a sizable positive absorption before the actual bleaching sets in. This absorption is most reasonably assigned to the phenoxyl radical, as discussed above. Furthermore, the overall decay kinetics exhibit principle features similar to those observed at 320 and 350 nm; that is, an initial fast process is followed by a slower one and also the same dependencies on  $[\text{Fe}(\text{CN})_6^{3-}]$ . (Quantitative analysis of the faster process was, however, not attempted because of the low signal intensity in the  $>400 \text{ nm}$  range).

A less ambiguous result, however, is obtained upon analysis of the slower part of the bleaching kinetics. The latter is clearly dependent on the  $\text{Fe}(\text{CN})_6^{3-}$  concentration as can be seen from a corresponding plot in Figure 5. From the slope of the straight line a second-order rate constant of  $(2.7 \pm 0.6) \times 10^6 \text{ M}^{-1} \text{ s}^{-1}$

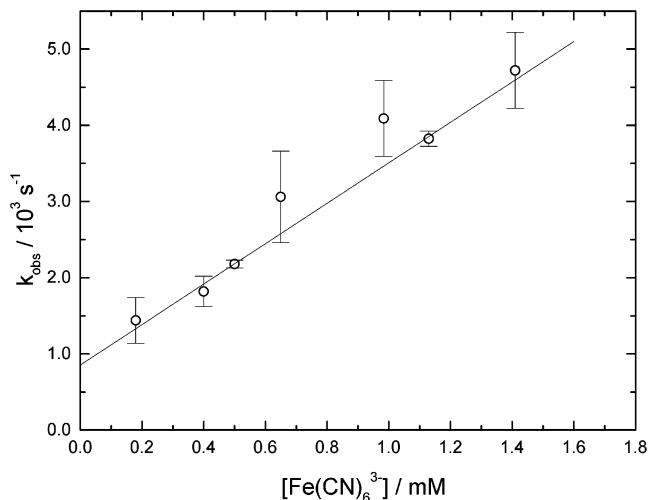


**Figure 5.**  $k_{\text{obs}}$  vs  $[\text{Fe}(\text{CN})_6^{3-}]$  for the “slow” decay part of the optical absorption traces measured at 420 nm (bleaching of  $\text{Fe}(\text{CN})_6^{3-}$ ) in pulse irradiated,  $\text{N}_2\text{O}$ -saturated aqueous solutions containing 3 mM TCP, pH 3.2–5.6.

was derived. This value is very close to the earlier estimation by Draper and also agrees with that attributable to the decay of the longer-lived part of 320 nm absorption in our current experiments. The latter was also accelerated by increasing  $\text{Fe}(\text{CN})_6^{3-}$  concentration. Although the absorption–time traces at 320 nm could not be fit fully satisfactorily by a single first-order exponential, the observed first half-lives closely matched those of the 420 nm slow bleaching process.

**Yields.** The total change of the absorption at 420 nm from the transient positive maximum to the final, negative bleaching value (Figure 4; i.e., during the time span from shortly after the pulse up to ca. 1.5 ms), amounts to  $(G \times \epsilon) = 7.0 \times 10^{-4} \text{ J}^{-1} \text{ cm}^{-1}$ . Based on our kinetic evaluation, about  $4.4 \times 10^{-4} \text{ J}^{-1} \text{ cm}^{-1}$  of this absorption change belongs to the slow process, whereas the remainder of about  $2.6 \times 10^{-4} \text{ J}^{-1} \text{ cm}^{-1}$  refers to the initial, fast decaying part. An unambiguous quantification of the  $\text{Fe}(\text{CN})_6^{3-}$  bleaching is, unfortunately, not possible because of the unknown contributions of the phenoxyl radical decay which includes the bimolecular termination of the latter and the possible cross reactions of this oxidizing radical with the various reducing species. Possible ground-state absorptions by final stable and as yet unknown products also have to be taken into consideration.

The total initial yield of reducing radicals in our system is given by the combined yields of  $\cdot\text{OH}$  radicals ( $G = 0.61 \mu\text{mol J}^{-1}$ ) and  $\text{H}^{\cdot}$  atoms ( $G = 0.06 \mu\text{mol J}^{-1}$ ), diminished by the yield of phenoxyl radicals (estimated to  $G = 0.14 \mu\text{mol J}^{-1}$ ), i.e.,  $G_{\text{red}} = 0.53 \mu\text{mol J}^{-1}$ . It may be worthwhile to examine this figure in light of two simplifying scenarios. The first assumes that the contribution of the phenoxyl radical to the total absorption does not diminish over the time interval of observation; that is, the entire signal decay is only due to bleaching of  $\text{Fe}(\text{CN})_6^{3-}$ . Taking the known extinction coefficient of  $\text{Fe}(\text{CN})_6^{3-}$  ( $\epsilon = 1020 \text{ M}^{-1} \text{ cm}^{-1}$ ) the above-mentioned total absorption change of  $(G \times \epsilon) = 7.0 \times 10^{-4} \text{ J}^{-1} \text{ cm}^{-1}$  would translate into a total yield of reducing species of  $G_{\text{red}} = 0.69 \mu\text{mol J}^{-1}$ . This considerably exceeds the above estimated yield of reducing species and that, in turn, means that the decay process definitely includes a contribution by phenoxyl radicals. The other, also simplifying scenario assumes that the positive absorption, assigned to the phenoxyl radicals, decays completely during the time span of observation. In this case, all of the reactions of reducing radicals with  $\text{Fe}(\text{CN})_6^{3-}$  are exclusively covered by

the net bleaching of the signal which, looking at Figure 4b, extrapolates to approximately  $(G \times \epsilon) = 3.5 \times 10^{-4} \text{ J}^{-1} \text{ cm}^{-1}$  or  $G_{\text{red}} = 0.35 \mu\text{mol J}^{-1}$ . This value, now, is considerably smaller than the estimated yield of reducing species. It, therefore, appears that the phenoxyl radicals do, indeed, partially decay in this time span but also that, correspondingly, the diminution of the positive part of the transient signal involves bleaching of  $\text{Fe}(\text{CN})_6^{3-}$ . This, then, nicely corroborates the conclusions drawn from the kinetic analysis.

Because the phenoxyl radicals would mostly disappear via radical–radical interactions, i.e., second order reactions, their contribution to the overall decay should predominantly show up in the slow process. Accordingly, the above evaluated 2.6:4.4 ratio of the fast vs slow portion of the overall decay gets closer to a 1:1 ratio for the fast vs slow reduction of  $\text{Fe}(\text{CN})_6^{3-}$ . In other words, the two types of reducing radicals seem to be formed at roughly equal yields.

**Identity of Reducing Radicals and  $\text{Fe}(\text{CN})_6^{3-}$  Reduction Mechanism.** The experimental observations concerning the  $\text{Fe}(\text{CN})_6^{3-}$  reduction described above can only be explained if more than one reducing dihydroxycyclohexadienyl radical is formed upon the  $\bullet\text{OH}$  radical attack on the TCP molecule. We will consider the two most probable ones, namely, the isomer  $\bullet\text{OH}$ -adducts at the C-3 and C-6 position, respectively, i.e., radicals **A** $\bullet$  and **B** $\bullet$  (Scheme 1). This choice is based on (i) electron density considerations which should be highest at these target carbons, (ii) the known electrophilic character of the  $\bullet\text{OH}$  radical, and (iii) the fact that these positions are sterically very accessible since they carry only hydrogen atoms as substituent. Furthermore, according to the AM1 calculations<sup>3</sup> the heat of formation of **A** $\bullet$  has been estimated to be more negative by about 5 kcal mol<sup>-1</sup> than that of **B** $\bullet$ .

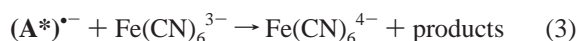
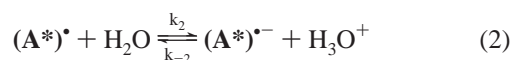
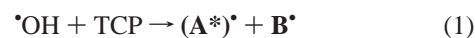
With respect to the redox properties, the rate constants for the  $\text{Fe}(\text{CN})_6^{3-}$  reduction by the isomers are relatively low and considerably below those for diffusion controlled electron-transfer processes.<sup>11</sup> This is related to the electron density withdrawing capacity of the chloro substituents. However, because both **A** $\bullet$  and **B** $\bullet$  carry the same number of chlorine atoms, we question whether this effect alone can explain the almost 2 orders of magnitude difference in the measured rate constants. A much more satisfying explanation is offered on the basis of (i) structural grounds, (ii) the pH and  $[\text{Fe}(\text{CN})_6^{3-}]$  dependencies of our present kinetic data (see Figure 3), and (iii) consideration of the  $\text{p}K_{\text{a}} = 4.8$  reported for **A** $\bullet$ .<sup>3</sup>

Structurally, the most significant feature of **A** $\bullet$ , as opposed to **B** $\bullet$ , is the adjacent location of the two hydroxyl groups. This provides the possibility for hydrogen bonding between the two respective oxygen atoms as depicted in structure (**A** $\bullet$ ) $\bullet$ . Also, as a consequence of that, the remaining free hydrogen should become much more acidic providing a plausible rationale for the relatively low  $\text{p}K_{\text{a}}$  of this radical, with the anionic form of this acid/base equilibrium being represented by (**A** $\bullet$ ) $\bullet^{-}$  (see Scheme 1 and eqs 1 and 2). Such a stabilization, particularly of an anionic form, is not possible in **B** $\bullet$ , and consequently, this radical is much less acidic. In fact, it is reasonable to expect the first  $\text{p}K_{\text{a}}$  of the hydroxyl groups in **B** $\bullet$  to be even higher (>7) than that of an OH group in the parent phenol. This is because the reduced aromaticity, which results upon any radical addition to a benzene ring system, cannot be compensated by steric and thermodynamic gains as in (**A** $\bullet$ ) $\bullet$  and (**A** $\bullet$ ) $\bullet^{-}$ .

Another fact that should be taken into consideration concerns the redox properties of radicals. It is well established that the anionic forms, because of increased resonance possibilities, are generally more powerful reductants than their neutral (proto-

nated) forms.<sup>11,12</sup> We, therefore, propose that the higher of the two rate constant for  $\text{Fe}(\text{CN})_6^{3-}$  reduction,  $(1.4 \pm 0.3) \times 10^8 \text{ M}^{-1} \text{ s}^{-1}$ , refers to the reaction of (**A** $\bullet$ ) $\bullet^{-}$  and the lower one,  $(2.7 \pm 0.6) \times 10^6 \text{ M}^{-1} \text{ s}^{-1}$ , to the reaction of **B** $\bullet$  in its neutral form. It would, of course, have been attractive to conduct direct experiments with the basic, i.e., anionic, form of **B** $\bullet$  as reductant as well, but unfortunately, this was impossible. At the high pHs necessary for such experiments, the parent chlorophenol, TCP, is already in its deprotonated phenolate form, changing completely the  $\bullet\text{OH}$  radical attack pattern on TCP.

Such an assignment eliminates the problem of the two-order-of-magnitude difference in rate constants between fast and slow  $\text{Fe}(\text{CN})_6^{3-}$  reduction because the reduction involves species that differ in redox potential and charge. It also provides an explanation for the plateau values for the first-order reduction rate constants in Figure 3. Accordingly, the  $[\text{Fe}(\text{CN})_6^{3-}]$  independent part of  $k_{\text{obs}}$  for the fast reaction is assumed to represent the deprotonation process (eq 2,  $k_2 \cong 2.8 \times 10^4 \text{ s}^{-1}$ ) which at  $\text{pH} < \text{p}K_{\text{a}}$  is slow enough to become the overall rate determining step at higher  $\text{Fe}(\text{CN})_6^{3-}$  concentrations. Having  $k_2$  it is, in principle, also possible to calculate  $k_{-2}$  ( $= k_2/K_2$ ). Because of the high uncertainty in Draper's published  $\text{p}K_{\text{a}}$  ( $4.8 \pm 1$ ), this figure, however, would span 2 orders of magnitude ( $\cong 10^8$ – $10^{10} \text{ M}^{-1} \text{ s}^{-1}$ ) preventing us from drawing any further meaningful and justifiable conclusions.



It should be noted that the direct oxidation of (**A** $\bullet$ ) $\bullet$  by  $\text{Fe}(\text{CN})_6^{3-}$  (eq 4), within the  $\text{Fe}(\text{CN})_6^{3-}$  concentration range used in this study, is not competitive with the two-step pathway involving the sequence of reactions in eqs 2 and 3. This arises from the constant yields of the fast and slow processes of bleaching at 420 nm and places the rate constant  $k_4$  close to or possibly even smaller than  $k_5$  for the reduction of  $\text{Fe}(\text{CN})_6^{3-}$  by **B** $\bullet$  (eq 5):



The  $\bullet\text{OH}$  radical adduct isomers exhibit different spectral characteristics. Considering the mechanistic aspects discussed above and arguments listed under "Optical Spectra", we assign absorptions in the 300–370 nm region shown in Figure 1 (curve 1a) to the composite spectrum of (**A** $\bullet$ ) $\bullet$ , **B** $\bullet$ , and **C** $\bullet$  radicals. Spectrum 1b, taken at the time when species (**A** $\bullet$ ) $\bullet$  had decayed almost completely (170  $\mu\text{s}$  after the pulse of irradiation), is ascribed to **B** $\bullet$ . Particularly, if the contribution of **C** $\bullet$  (spectrum 1c) is subtracted from spectrum 1b, it exhibits only a single maximum at 320 nm. The (**A** $\bullet$ ) $\bullet$  isomer, on the other hand, clearly displays two, approximately equally intensive, maxima at about 320 and 350 nm (difference spectrum between 1a and 1b, not shown). It seems reasonable to take the additional red-shifted band at 350 nm as supportive evidence for the hydrogen bridged structure of this species.

In conclusion, our reinvestigation of the  $\bullet\text{OH}$  radical reaction with TCP has revealed, in contrast to the earlier study, the unambiguous existence of two different  $\bullet\text{OH}$ -adducts, namely, at the C-6 and C-3 positions, respectively. They appear to be

formed at about equal yield, exhibit different optical absorption spectra, and both are mild reductants as can be deduced from their reaction with  $\text{Fe}(\text{CN})_6^{3-}$ . Owing to its relatively low  $\text{p}K_a$  (4.8), the C-6-adduct in neutral to slightly acid solutions reacts preferentially through its deprotonated, anionic form. It can further be concluded that the C-6-adduct gains particular stability through hydrogen bond bridging between the two C-6- and C-1-positioned hydroxyl groups.

**Acknowledgment.** The financial support provided for M.B. through Northwestern University (NU) Institute of Environmental Catalysis funded by NSF with matching grants from NU and DOE (CHE-9810378) is gratefully acknowledged. The authors are also indebted to the Radiation Laboratory at Notre Dame and the U.S. Department of Energy for the possibility to use its Pulse Radiolysis facility. K-D.A. is currently on sabbatical leave from the Department of Chemistry of the University of Notre Dame.

## References and Notes

- (1) Schuler, R. H.; Neta, P.; Zemel, H.; Fessenden, R. W. *J. Am. Chem. Soc.* **1976**, *98*, 3825.
- (2) Getoff, N.; Solar, S. *Radiat. Phys. Chem.* **1986**, *28*, 443.
- (3) Draper, R. B.; Fox, M. A.; Pelizzetti, E.; Serpone, N. *J. Phys. Chem.* **1989**, *93*, 1938.
- (4) Terzian, R.; Serpone, N.; Draper, R. B.; Fox, M. A.; Pelizzetti, E. *Langmuir* **1991**, *7*, 3081.
- (5) Stafford, U.; Gray, K. A.; Kamat, P. V. *J. Phys. Chem.* **1994**, *98*, 6343.
- (6) Shoute, L. C. T.; Mittal, J. P.; Neta, P. *J. Phys. Chem.* **1996**, *100*, 3016.
- (7) *Environmental Applications of Ionizing Radiation*, Cooper, W. C., Curry, R. D., O'Shea, K. E., Eds.; J. Wiley & Sons: New York, 1998.
- (8) Hug, G. L.; Wang, Y.; Schöneich, C.; Jiang, P.-Y.; Fessenden, R. W. *Radiat. Phys. Chem.* **1999**, *54*, 559.
- (9) Schuler, R. H.; Hartzell, A. L.; Behar, B. *J. Phys. Chem.* **1981**, *85*, 192.
- (10) Janata, E.; Schuler, R. H. *J. Phys. Chem.* **1982**, *86*, 2078.
- (11) von Sonntag, C. *The Chemical Basis of Radiation Biology*; Taylor & Francis: New York, 1987.
- (12) Wardman, P. *J. Phys. Chem. Ref. Data* **1989**, *18*, 1637.